Microdiffraction Study Of Iron-Containing Nanotube Carpets

Pichot V. [1], Launois P. [1], Pinault M. [2], Mayne-L'Hermite M. [2], Reynaud C. [2], Burghammer M. [3], Riekel C. [3]

[1] *Laboratoire de Physique des Solides (UMR CNRS 8502), bât. 510, Université Paris Sud, 91405 Orsay Cedex, France*

[2] *Laboratoire Francis Perrin (URA CNRS 2453), CEA Saclay, DRECAM-SPAM, bât. 522, 91191 Gif sur Yvette, France*

[3] *The European Synchrotron Radiation Facility (ESRF), 6 rue Jules Horowitz, 38043 Grenoble, France*

Abstract. X-ray microdiffraction can be a powerful technique to study nanotube-based materials, as shown here for carpets of aligned multiwall carbon nanotubes synthesized by aerosol-assisted Catalytic Chemical Vapor Deposition. Catalytic particles are found to be iron oxide. Moreover, local analysis of nanotube alignment allows one to understand the effects of the synthesis procedure.

Keywords: Nanotubes, X-ray diffraction, aerosol-assisted Chemical Vapor Deposition
PACS: 61.46.+w, 61.10.Nz, 81.15.Gh

INTRODUCTION

The synthesis of macroscopic nanotube (NT) carpets of several cm^2, composed of mm long nanotubes aligned perpendicularly to the surface of a substrate is a challenge for many applications, from high density magnetic storage [1] to chemical separation [2]. Special interest is focused on Catalytic Chemical Vapor Deposition (CCVD) methods for low cost and large scale production [3]. However, recent experiments [4,5] showed that the structure of carpets could vary from their basis to their top, which is of course a crucial point for future applications. Therefore local analyses are needed in order to characterize in details carpet structure and subsequently to better control the synthesis methods. In this context, we performed X-ray microdiffraction experiments. To our knowledge, it is the first time that X-ray microdiffraction is used for the study of a nanotube-based material.

EXPERIMENTS

Carpets of aligned multi-wall carbon nanotubes (MWNT) were synthesized by CCVD of liquid aerosol obtained from toluene/ferrocene (5 wt. %) solution [6]. The experimental set-up is composed of an aerosol generator, a quartz reactor placed in a

furnace and traps for the gases coming out. Synthesis is performed on thin silicon wafers (covered by a SiO_2 native layer) placed in the reactor heated at 850°C and fed during 15 min with the aerosol carried by argon gas. The quartz reactor is then slowly cooled down to room temperature. Two different experimental set-ups were used [7]. Our initial experimental set-up was composed of a single argon inlet. When stopping the aerosol generation and starting cooling, the argon gas flushes the remaining aerosol to the reactor. Aerosol characteristics (density, ferrocene concentration,…) are no more controlled. The experimental device has been improved by changing the argon distribution through the addition of a second argon inlet : aerosol feeding can be stopped instantaneously by sending a high argon flow through the additional inlet. Carpet 1 (C1) was obtained with the initial set-up and carpet 2 (C2) with the modified one; their thicknesses are about 600µm and 500µm, respectively.

X-ray microdiffraction experiments, with maximum beam size of 2µm x 2µm, were performed using high flux synchrotron radiation at ESRF (beamline ID13, wave-length 0.9755Å). The small beam size allowed us to analyze the carpet from its bottom to its top; fig. 1 inset details the geometry of the experiment. Diffraction patterns are recorded on a two-dimensional CCD detector. They exhibit scattering rings whose positions allow one to determine the structure of the scattering objects and whose modulations characterize preferential orientations if any.

RESULTS AND DISCUSSION

Analysis of diffraction patterns recorded from the bottom of carpets C1 and C2 (next to the wafer) to their top shows the occurrence of an iron oxide phase -magnetite Fe_3O_4 or isostructural maghemite γ-Fe_2O_3- mainly located just above the wafer. This is illustrated in fig. 1 where the intensity of the most intense diffraction peak of magnetite (or maghemite) is plotted as a function of the beam position with respect to the wafer. These microdiffraction results, together with X-Ray Photoelectron Spectroscopy and Transmission Electron Microscopy/Energy Dispersive X-ray results discussed in ref. [7], demonstrate that catalytic particles are iron oxide. Nanotube formation occurs through a base growth mechanism from these particles [6,7]. To our knowledge, only one result has been published in the literature for carpets obtained by CCVD of prevaporised hydrocarbon (xylene) / ferrocene solutions, which reports the occurrence of γ–Fe [8]. Note also that few papers give experimental evidence for the growth of nanotube or filamentous carbon from iron oxide by CCVD of hydrocarbon gas [9-11]. In most cases, catalytic particles are iron or iron carbide. For discussion of our result, beyond the scope of this article, the reader should refer to ref. [7]. Our aim here is to show that microdiffraction is a powerful tool to obtain local information about iron-based phases in NT carpets (catalytic particles, as shown here, but also nanowires inside NTs).

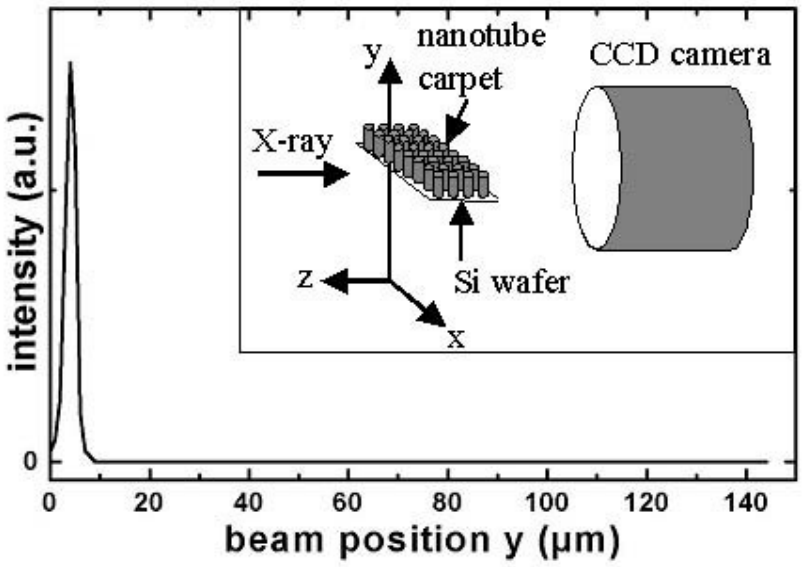

FIGURE 1. Intensity of the (3,1,1) peak of cubic magnetite (or of isostructural maghemite) at 2.5$Å^{-1}$, for carpet C1, as a function of the beam position y with respect to the silicon wafer (the wafer surface corresponds to y≈0, results shown here are for the 150 μm above the wafer). Inset: the normal to the carpet basis is placed perpendicular to the X-ray beam, its width Δz along the X-ray beam being chosen to be rather small (~0.2mm) to preserve good resolution. The structural information obtained for beam position (x,y) concerns the parallelepiped defined by the beam on the carpet (2μm x 2μm x Δz). Intensity as a function of y is obtained by translating the carpet perpendicularly to the beam at a constant x position.

Information about the nanotube orientation around the normal to the carpet basis is obtained from the angular modulation of the (002) MWNT diffraction peak at 1.83$Å^{-1}$. As explained in ref. [4], it is characterized by its Half-Width at Half Maximum (HWHM), which is displayed in fig.2. Figure 2 shows that nanotube orientation is roughly the same (+/- 15° with respect to the normal of the carpet base) in the core of carpets C1 and C2, sufficiently far away from the substrate. However, such alignment degree is strongly disturbed over 50 μm above the wafer for carpet C1 (+/- 30° alignment value is measured close to the wafer). The different alignment degrees are related to the synthesis procedures used. Considering that growth occurs from nanotube basis, the low alignment degree at the basis of carpet C1 is attributed to the changes in ferrocene concentration and in aerosol density during the stopping procedure. On the contrary, the alignment degree at the basis of carpet C2 is not affected since the aerosol is suddenly stopped. Such results illustrate the crucial role of synthesis procedure on carpet structure.

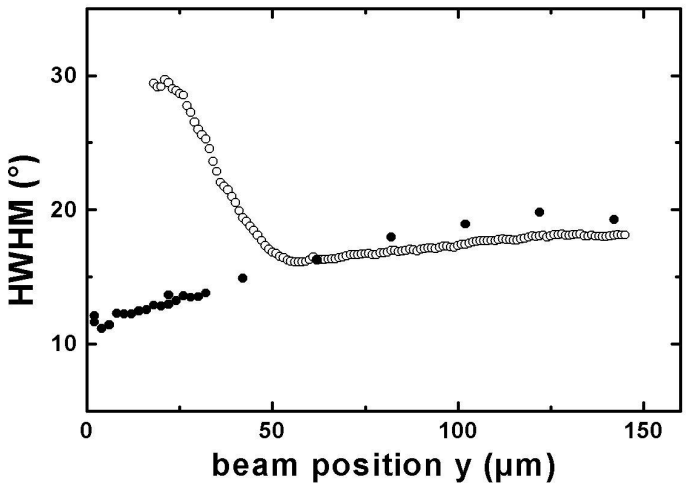

FIGURE 2. HWHM of the (002) NT peak modulation for carpets C1 (open circles) and C2 (filled circles) over the first 150 µm above the silicon wafer (wafer's surface corresponds to y≈0); note that due to absorption effects, data analysis could not be performed very close to the wafer for carpet C1.

ACKNOWLEDGMENTS

This work has been done thanks to collaborations established in the framework of the CNRS GDR n° 1752 'Nanotubes mono- et multi-éléments' and of the GDRE n°2756 'Science and applications of the nanotubes - NANO-E'. FIT2D program provided by A.P. Hammersley and the ESRF was used for the data analysis.

REFERENCES

1. Grobert N., Hsu W.K., Zhu Y.Q., Hare J.P., Kroto H.W., Walton D.R.M., Terrones M., Terrones H., Redlich Ph., Rulhe M., Escudero R., Morales F., *Appl. Phys. Lett*. **75**, 3363-3365 (1999)
2. Hinds B.J., Chopra N., Rantell T., Andrews R., Gavalas V., Bachas L.G., *Science* **303**, 62-65 (2004)
3. Singh C., Shaffer M.S.P., Koziol K.K.K., Kinloch I.A., Windle A.H., *Chem. Phys. Lett.* **372**, 860-865 (2003)
4. Pichot V., Launois P., Pinault M., Mayne-L'Hermite M., Reynaud C., *Appl. Phys. Lett.* **85**, 473-475 (2004)
5. Ruskov T., Asenov S., Spirov I., Garcia C., Mönch I., Graff A., Kozhuharova R., Leonhardt A., Mühl T., Ritschel M., Schneider C.M., Groudeva- Zotova S., *J. Appl. Phys.* **96**, 7514-7518 (2004)
6. Pinault M., Mayne-L'Hermite M., Reynaud C., Beyssac O., Rouzaud J.N., Clinard C., *Diamond and related materials* **13**, 1266-1269 (2004)
7. Pinault M., Mayne-L'Hermite M., Reynaud C., Pichot V., Launois P., Ballutaud D., submitted
8. Jung Y.J., Wei B., Vajtai R., Ajayan P.M., Homma Y., Prabhakaran K. and Ogino T., *Nano Lett*. **3**, 561-564 (2003)
9. Fan S., Chapline M.G., Franklin N.R., Tombler T.W., Cassell A.M., Dai H., *Science* **283**, 512-514 (1999)
10. Baker R.T.K., Alonzo J.R., Dumesic J.A., Yates D.J.C., *J. of Catalysis* **77**, 74-84 (1982)
11. Mauron Ph., Emmenegger C., Züttel A., Nützenadel Ch., Sudan P., Schlapbach L., *Carbon* **40**, 1339-1344 (2002)